

# Near-future extreme sea level predictions from physics-informed deep networks

Anonymous Full Paper  
Submission 6

## Abstract

Storm surges, high-frequency extreme sea level events driven by the atmosphere, lead to loss of life and crucial infrastructure. Their prediction is a requirement to build adequate coastal protection, yet by design the current generation of coupled climate models cannot reliably do so. They have however long been used to predict and project changes in the atmosphere. We here re-train a recently produced physics-informed Long Short Term Memory (LSTM) network that was designed to reproduce observed extreme sea level events around Northern Europe. We notably reduce its number of predictors to the six atmospheric variables that the network ranked as most important and its temporal resolution from hourly to 3-hourly, so that we can pass as predictors climate model-produced atmospheric variables. We compare the climate model-based and observed sea level over 1985-2014 and select the most accurate runs to quantify changes in the number of extreme sea level events in the near-future (2025-2054) and end of century (2070-2099). The network projects on average increases in the number of extreme events, but there is a large spread in the predictions. In general, it also projects a larger increase in the near-future than at the end of the century. We attribute this spread to the inconsistent changes in the drivers: larger wind speeds, shifting from more west-northerly in the near-future to more west-southerly at the end of the century, yet higher sea level pressure. These results show the feasibility of predicting changes in extreme events from physics-informed deep learning networks, but more reliable predictors, from a wider range of climate models, are needed before the predictions can converge.

## 1 Introduction

Northern Europe is particularly vulnerable to extreme sea level events, as most of its population, financial and logistical hubs are located by the coast [1]. These events are expected to increase as climate change continues [2], but the exact numbers are uncertain. One main reason for this uncertainty is that our usual tool for climate change predictions and projections, global climate models, cannot -by design- reproduce accurate sea level [3]: Because notably of their vertical grid, the sea surface is often fixed

and calculated afterwards, prognostically. They can however reproduce atmospheric processes [4], and we know that over Northern Europe, extreme sea level events are atmosphere-driven [2].

Using machine learning to predict extreme sea level events from atmospheric drivers is a logical next step. Using neural networks, Hieronymus et al. [5] could show that 36h forecasts for the Swedish coast were as accurate and much faster to produce than traditionally done with hydrodynamics models. Dubois et al. [6] extended their work and produced sea level predictions for the Baltic coast for the entire 21st century with Random Forest. More computationally demanding but more accurate, Barzandeh et al. [7] used an encoder-based deep network to predict extreme sea level along the coast of Estonia, while Heuzé et al. [8] used instead a Long Short Term Memory (LSTM) recurrent neural network, applying it to stations along the North Sea and Baltic coasts. These deep learning works focussed on reproducing and explaining observed sea level, rather than projecting long term changes.

Using transfer learning, we here re-train the LSTM network developed by Heuzé et al. [8] so that it can provide extreme sea level projections for stations around Northern Europe. Using an approach similar to that of Dubois et al. [6], we use as predictors outputs produced by the climate models that participated in the Climate Model Intercomparison Project phase 6 [CMIP6, 4]. After an assessment of the performances of this approach by comparing observed and climate model-inferred sea level over the historical period, we quantify changes in extreme sea level events for the near-future (2025 - 2054) and the end of the century (2070 - 2099).

## 2 Data and Methods

The Zenodo link and DOI of the scripts necessary to reproduce our results will be provided in the camera-ready version.

### 2.1 Sea level and atmospheric observational datasets

We use hourly tide gauge data from the same nine stations around Northern Europe as used by Heuzé et al. [8]: Den Helder (NL), Esbjerg (DK) and Lowestoft (UK) on the North Sea coast; Gedser (DK),

092 Helsinki (FI) and Umeå (SWE) on the Baltic coast;  
093 and Gothenburg (SWE), Malmö (SWE) and Oslo  
094 (NO) in the transition between the two seas. For  
095 the three Swedish cities Gothenburg, Malmö and  
096 Umeå, the tide gauge data were provided by the  
097 Swedish Meteorological and Hydrological Institute;  
098 for the other locations, we used the Global Extreme  
099 Sea Level Analysis (GESLA) dataset version 3, last  
100 updated in November 2021 [9, 10]. We de-tided the  
101 tide gauge data using the UTide package for Matlab  
102 [11], keeping the trends in.

103 The observed atmospheric variables used to train  
104 the network are from the ERA5 reanalysis [12],  
105 available at 0.25° resolution, hourly, since 1st Janu-  
106 ary 1940. We use the hourly 10 m  $u$ - and  $v$ -  
107 components ( $u_{10}$  and  $v_{10}$ ) of the wind and the mean  
108 sea level pressure, at the grid cell closest to the tide  
109 gauge station coordinates as provided by SMHI or  
110 GESLA. We further computed the wind speed as  
111  $WS = \sqrt{u_{10}^2 + v_{10}^2}$ , and split the wind components  
112 into their positive (i.e. westerly or southerly) and  
113 negative (i.e. easterly or northerly) components.

114 The highest temporal resolution available for  
115 CMIP6 models is 3-hourly; we therefore retimed  
116 all our hourly series, producing 3-h bin mean values  
117 with bins including times 0,1,2h, 3,4,5h etc, to be  
118 consistent with the CMIP6 times.

## 119 2.2 Output from the Climate Model 120 Intercomparison Project phase 6

121 We use all CMIP6 models that at the time of down-  
122 load (June 2025) had the 3-hourly 10 m  $u$ - and  $v$ -  
123 components of the wind and the mean sea level pres-  
124 sure ('uas', 'vas', and 'psl' respectively in the CMIP  
125 nomenclature) for the historical run and at least  
126 one of the climate change runs. This amounted to  
127 exactly two models, from the same modelling family:  
128 MPI-ESM1-2-LR and MPI-ESM-1-2-HAM [13]. We  
129 acknowledge that this is not representative of the  
130 CMIP-model potential for such projection, and can  
131 only hope that future iterations of CMIP will feature  
132 more models with high temporal resolution output.

133 We chose the Shared Socioeconomic Pathway 3-  
134 7.0 as for these models, it was the one with the most  
135 ensemble members available [datasets 14–17]. In  
136 total, for both experiments, we have 50 ensemble  
137 members for MPI-ESM1-2-LR (51 for the historical  
138 run) and 3 for MPI-ESM-1-2-HAM; we use them  
139 all in the historical assessment, and limit our future  
140 projections to the 10 best performing of both models  
141 considered together. We assessed their performance  
142 by ranking the models based on their ability to  
143 reproduce the observed 99th percentile in sea level,  
144 for all nine cities, and taking the ten with the lowest  
145 combined rank.

146 For all climate models and ensemble members, for  
147 each city, we extracted the wind and pressure values

of the grid cell closest to the city's tide gauge coordi-  
nates. As for the observations, we also compute the  
wind speed and decompose the wind components into  
their north/south/east/westerly contributions. We used  
those as predictors for our deep network, as described  
in the next section, to produce sea level values. We  
quantify biases in these re-created sea level values  
on the last 30 years of the historical run (1 January  
1985 to 31 December 2014) and perform the sea level  
projections over the 30-year periods “near-future”  
(1 January 2025 - 31 December 2054) and “end of  
century” (1 January 2070 - 31 December 2099).

## 2.3 Long Short Term Memory and its re-training

We re-use the model architecture of Heuzé et al. [8],  
which they provided at <https://doi.org/10.5281/zenodo.15754554>. In brief, a deep network  
was trained to reproduce extreme sea level around  
Northern Europe from atmospheric predictors. This  
network is a Long Short Term Memory [LSTM, 18],  
which is a type of recurrent neural network that can  
take complex temporal dependencies into account. The  
LSTM, based on the Python package Keras [19], has  
3 layers of 100 units each with a hyperbolic tangent  
activation function, and one dense layer, with a drop  
out rate of 0.015 in between each layer, an overall  
learning rate of 0.01, and 12h windows. For the  
original hourly predictors, the input batch size was  
20; for our 3-hourly predictors, we use a batch size  
of 7.

We not only reduced the temporal resolution from  
hourly to 3-hourly, we also reduced the number of  
predictors to the six that were deemed most impor-  
tant for the region [8]: the 4 wind components, the  
wind speed, and the sea level pressure. We could  
directly re-use the same LSTM architecture and ob-  
tain great performances (Fig. 1): correlation larger  
than 0.9 with the observed sea level, and overall  
RMSE of 0.04, reduced to 0.02 or less for the high  
values (larger than 0.66 when normalised).

All datasets, be they from observations or CMIP6  
models, are min-max normalised prior to feeding to  
the LSTM.

## 3 Results and Discussion

### 3.1 Historical assessment

We first use the 3-hourly CMIP6 outputs of sea level  
pressure and winds for 1985-2014 as predictors in  
our network, and compare their produced sea level  
to that from tide gauge observations over the same  
time period. We focus on the 99th percentile of the  
time series, which over 30 years of 3-hourly data  
yields 877 events.

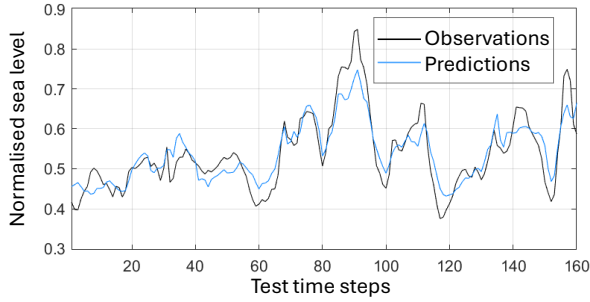


**Figure 1.** Performance of the LSTM prediction (blue) against its test set (black), for tide gauge observations from Gothenburg, roughly at the centre of the region of interest.

201 The performances of the best and worst ensemble  
 202 members are shown for each city, for the two CMIP6  
 203 models, in Table 1. Starting with the best runs,  
 204 we find that six of the locations have the correct  
 205 value of their 99th percentile over the historical  
 206 level, with biases in the number of events in that  
 207 percentile lower than 1%. The other three cities  
 208 have biases lower than 10% for MPI-ESM1-2-LR,  
 209 worsening to nearly 14% for MPI-ESM-1-2-HAM,  
 210 i.e. the observed highest 1% of the sea levels occur  
 211 15% of the time in the model. Performances are  
 212 somewhat consistent across the ensemble members.  
 213 That is, if the best run has a low bias, so does the  
 214 worst run (Table 1): the six cities we highlighted  
 215 previously reach at most 5% error for their worst  
 216 run, while Den Helder, Esbjerg and Gothenburg  
 217 have 5 to 18% bias. As expected, the range best-  
 218 to-worst is smaller across the 3 ensemble members  
 219 of MPI-ESM-1-2-HAM than across the 51 of MPI-  
 220 ESM1-2-LR (0.1-2.5% vs 1-10%).

221 Parts of these biases and their spread most likely  
 222 stem from differences in the distribution of the  
 223 drivers. Looking again at Gothenburg, which is  
 224 in the centre of our region of interest and one of the  
 225 cities with higher biases, we find that both the best  
 226 and worst ensemble members have their mean sea  
 227 level pressure shifted low compared to the reanalysis  
 228 (Fig. 2a), with the shift more severe for the worst  
 229 performing models. The modelled u-wind simulta-  
 230 neously has too few low (-5 to 0 m/s) and too many  
 231 high (-15 to -5 m/s) easterly values, with the worst  
 232 run also having too wide a distribution for the low  
 233 westerly values (Fig. 2b). The modelled v-wind is  
 234 centered on 0 m/s and has a symmetric distribution,  
 235 while the observed has a southerly shift; if anything,  
 236 the best performing run seems to be most biased.  
 237 That is, predictor biases across ensemble members  
 238 are inconsistent.

239 Interestingly, not one single ensemble member is  
 240 best in all cities, even for MPI-ESM-1-2-HAM that  
 241 has only 3 to choose from. For the climate change  
 242 analysis, for each city, we therefore rank all ensemble

**Table 1.** Best and worst runs of the two CMIP6 models, i.e. minimum and maximum biases. For each city, First column: 99th percentile sea level in the observations and corresponding value when the series is min-max normalised; Second, minimum percentile difference, in %, corresponding to that value (0 if it is the 99th percentile for the model too, positive bias if that sea level value is more common in the model); Last column, maximum difference in % in percentile corresponding to that value. ‘LR’ and ‘HAM’ refer to the two CMIP6 models MPI-ESM1-2-LR and MPI-ESM-1-2-HAM, respectively. Second row is the run number of the corresponding ensemble member, in the CMIP6 format r[run number]i1p1f1.

City	Obs 99 prct (min-max norm.)	Best run		Worst run	
		LR	HAM	LR	HAM
DeH	0.89 m (0.59)	8.8 46	13.9 3	18.1 31	16.5 1
Esb	1.22 m (0.6)	6.1 28	9.5 3	11.9 13	10.9 2
Ged	0.59 m (0.71)	0.0 11	0.0 1	1.5 13	0.5 2
Got	0.58 m (0.62)	2.6 33	3.6 2	7.3 30	4.8 1
Hel	0.62 m (0.67)	0.6 42	0.5 3	2.5 15	1.8 2
Low	0.68 m (0.69)	-0.1 37	1.0 3	3.0 31	2.1 2
Mal	0.47 m (0.68)	0.5 22	1.2 1	3.8 20	2.3 2
Osl	0.65 m (0.61)	-0.2 42	0.7 2	4.6 2	5.2 3
Ume	0.64 m (0.71)	0.1 15	-0.3 1	-0.8 14	-0.4 3

members based on their bias, combining the two 243  
 CMIP6 models, and then take their median rank 244  
 across all nine cities. We ignore r2000i1p1f1, which 245  
 is not available for the future runs. We take the 10 246  
 with the lowest median rank, which corresponds to 247  
 an average rank strictly lower than 20 (out of 54), 248  
 and analyse their predictions in the next section. 249  
 These 10 all belong to MPI-ESM1-2-LR, and are 250  
 (best first): r40, 18, 7, 22, 48, 12, 50, 11, 46, and 251  
 17i1p1f1. 252

### 3.2 Near-future and end-of-century extreme sea level events 253 254

The LSTM network predicts a large range of changes 255  
 in sea level extremes even after selecting for the 10 256  
 best ensemble members (Table 2). On average, it 257  
 predicts an increase in the number of events, except 258  
 for Umeå where they will decrease. Five (four) of 259  
 the cities have a median change stronger (lower) in 260  
 the near future than by the end of the century. For 261  
 all cities, except Umeå in the near-future, the most 262  
 extreme predictions are of opposite sign. That is, de- 263  
 spite a projected increase on average, there is at least 264  
 one ensemble member that predicts a decrease. In 265

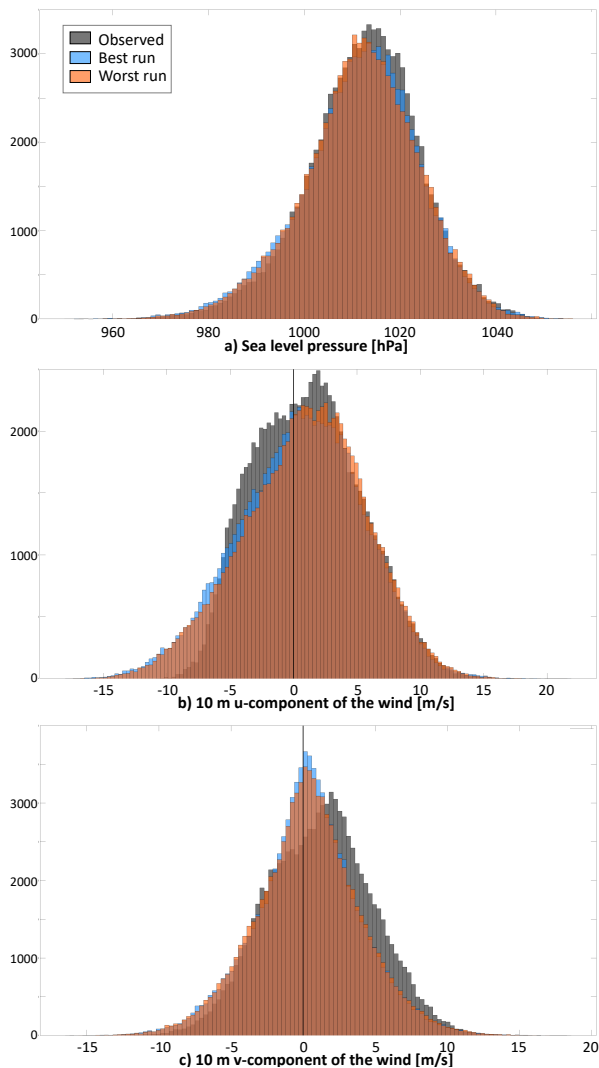


**Figure 2.** Distribution of the three 3-hourly atmospheric variables over 1985-2014 for Gothenburg, in observations (grey), in the best (blue) and worst (orange) performing ensemble member according to Table 1.

266 general, this projected possible decrease is stronger  
267 in the near-future than for the end of the century,  
268 but so is also the projected maximum increase. That  
269 is, as has been shown for other variables [e.g. 20],  
270 the internal variability becomes relatively weaker as  
271 the climate change forcing increases.

272 The reason for this range of predictions proba-  
273 bly is the inconsistent changes in the atmospheric  
274 drivers (Fig. 3). The sea level pressure (a) is shifting  
275 towards higher values, i.e. less stormy conditions,  
276 which would be consistent with predictions of fewer  
277 extreme events. The winds in contrast are shifting  
278 away from 0. The u-component (b) is becoming  
279 more westerly, which over northern Europe means  
280 stormier conditions and therefore more extreme sea  
281 level events. The v-component shifts northerly, i.e.  
282 stormier, in the near-future (Fig. 3c, green), and  
283 then shifts southerly by the end of the century (pur-  
284 ple). These are consistent with the stronger in-

**Table 2.** Change in the number of events with sea level higher than the observed 99th percentile (from Table 1) between the near future (2025-2054) and the end of century (2070-2099) compared to the historical period. Table shows the minimum, median and maximum across the 10 ensemble runs.

City	2025 - 2054			2070 - 2099		
	min	median	max	min	median	max
DeH	-7231	670	5554	-4228	1662	4568
Esb	-2676	915	3888	-390	1000	4570
Ged	-286	293	895	-391	185	741
Got	-2500	1241	3333	-2294	1063	2964
Hel	-1242	35	897	-574	124	785
Low	-1356	8	1715	-1202	210	1276
Mal	-293	713	1777	-480	547	1174
Osl	-2393	1373	2116	-2921	542	2617
Ume	-404	-160	-62	-338	-4	404

crease in the near-future. Earlier results [8] had  
also pointed out that Umeå was the one location  
where southerly winds were important predictors:  
this end-of-century southerly shift probably explains  
the emergence of predictions with increased extreme  
sea level events for that city (Table 2, bottom right  
cell).

Which atmospheric change is the correct one?  
The sea level pressure is less biased than the wind  
components (Fig. 2), so its projections of decreased  
storminess ought to be more trustworthy, but most  
literature on climate change anticipate more storms  
[21]. Ideally, one would have access to more CMIP6  
models, from diverse modelling centres, and would  
select only those with accurate atmospheric drivers.  
Unfortunately only two models, from the same model  
family, released the 3-hourly output needed for this  
study. The upcoming CMIP7 [22] is putting a large  
emphasis on studying extreme events, so we can  
hope that more model output will become available  
soon for this type of work. Given that a recent study,  
using different CMIP output and Random Forest,  
found a similarly large range predictions [6], a better  
option may be to work with bias-corrected output,  
although correcting related output with opposite  
biases is not trivial.

Finally, it is important to bear in mind that this  
is only the atmosphere-induced part of extreme sea  
level events. In reality, the baseline of sea level is  
shifting [2], and waves and tides are changing too  
[23]. Even if the atmosphere were to become more  
stable and cause fewer extreme sea level events, these  
other processes will still increase the vulnerability  
of our coastlines [1].

## 4 Conclusion

We re-trained a Long Short Term Memory network  
that had been designed specifically to reproduce

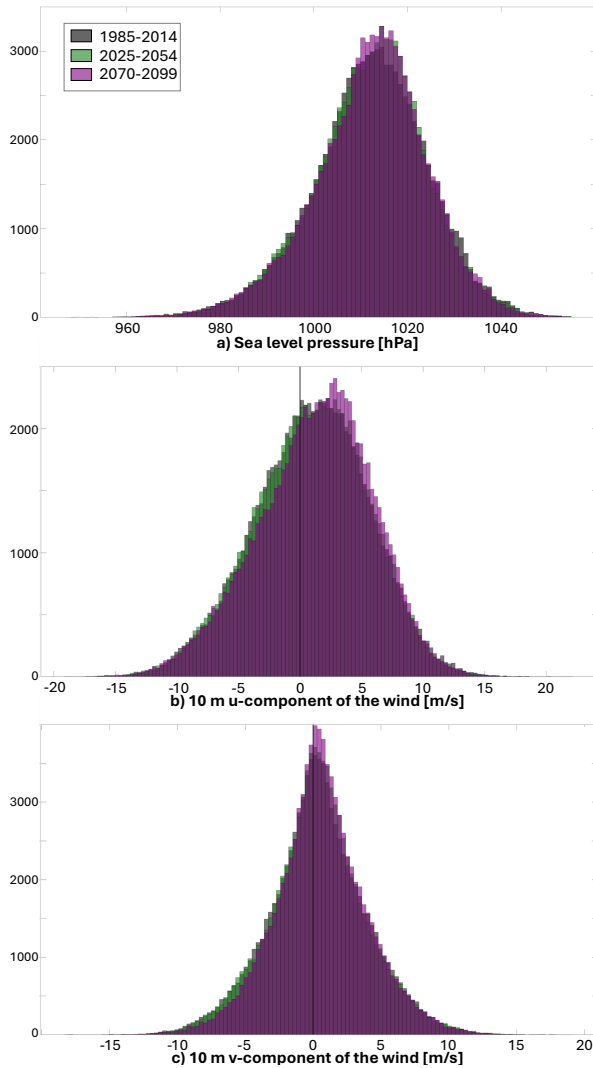


**Figure 3.** Distribution of the three 3-hourly atmospheric variables for Gothenburg for the historical period 1985-2014 (black), the near-future 2025-2054 (green), and the end of century 2070-2099 (purple).

extreme sea level around Northern Europe [8], so that it can now take as predictors climate model-produced atmospheric variables instead of the original observational datasets. That is, we reduced the number of predictors to the four wind components (northerly, southerly, westerly, easterly), wind speed, and sea level pressure, coming from three climate model-produced variables, and reduced the temporal resolution from hourly to the model-outputted 3-hourly. We used all models and all ensemble members that had these three variables available for the historical and climate change run SSP3-7.0, which amounted to only two models from the same model family and 54 ensemble members. We selected the 10 ensemble members that produced the most accurate historical extreme sea level (Table 1), and found an overall increase in the number of extreme sea level events in the future (Table 2) but with a large range of uncertainty. This is because the dif-

ferent atmospheric variables have large biases (Fig. 2) and surprising opposite changes (Fig. 3). As sea level keeps rising in response to sustained climate change, the risk of extreme events will only increase [2]. Such predictions are therefore urgently needed, and urgently need to become less uncertain, for example by increasing the number of models that release 3-hourly output [22].

## Acknowledgments

This work was funded by [anonymised] grant no. [anonymised] awarded to [anonymised]. We acknowledge the World Climate Research Programme, which, through its Working Group on Coupled Modelling, coordinated and promoted CMIP6. We thank the climate modeling groups for producing and making available their model output, the Earth System Grid Federation (ESGF) for archiving the data and providing access, and the multiple funding agencies that support CMIP6 and ESGF. We acknowledge the data access and computing support provided by [anonymised].

## References

- [1] R. van de Wal, A. Melet, D. Bellafiore, P. Camus, C. Ferrarin, G. Oude Essink, I. Haigh, P. Lionello, A. Luijendijk, A. Toimil, and J. Staneva. “Sea Level Rise in Europe: Impacts and consequences”. In: *State of the Planet 3* (2024), pp. 1–33. DOI: [10.5194/sp-3-slre1-5-2024](https://doi.org/10.5194/sp-3-slre1-5-2024).
- [2] A. Melet, R. van de Wal, A. Amores, A. Arns, A. Chaigneau, I. Dinu, I. Haigh, T. Hermans, P. Lionello, M. Marcos, and H. Meier. “Sea level rise in Europe: Observations and projections”. In: *State of the Planets 4* (2024). DOI: [10.5194/sp-3-slre1-4-2024](https://doi.org/10.5194/sp-3-slre1-4-2024).
- [3] S. M. Griffies, G. Danabasoglu, P. J. Durack, A. J. Adcroft, V. Balaji, C. W. Böning, E. P. Chassignet, E. Curchitser, J. Deshayes, H. Drange, et al. “OMIP contribution to CMIP6: Experimental and diagnostic protocol for the physical component of the Ocean Model Intercomparison Project”. In: *Geoscientific Model Development* 9.9 (2016), pp. 3231–3296. DOI: [10.5194/gmd-9-3231-2016](https://doi.org/10.5194/gmd-9-3231-2016).
- [4] V. Eyring, S. Bony, G. A. Meehl, C. A. Senior, B. Stevens, R. J. Stouffer, and K. E. Taylor. “Overview of the Coupled Model Intercomparison Project Phase 6 (CMIP6) experimental design and organization”. In: *Geoscientific Model Development* 9.5 (2016), pp. 1937–1958. DOI: [10.5194/gmd-9-1937-2016](https://doi.org/10.5194/gmd-9-1937-2016).

- [5] M. Hieronymus, J. Hieronymus, and F. Hieronymus. “On the application of machine learning techniques to regression problems in sea level studies”. In: *Journal of Atmospheric and Oceanic Technology* 36.9 (2019), pp. 1889–1902. DOI: [10.1175/JTECH-D-19-0033.1](https://doi.org/10.1175/JTECH-D-19-0033.1).
- [6] K. Dubois, E. Nilsson, M. D. D. Andreas, M. Hieronymus, P. Karami, A. Rutgersson, et al. “Exploring Storm Tides Projections and Their Return Levels Around the Baltic Sea Using a Machine Learning Approach”. In: *Tellus. Series A, Dynamic meteorology and oceanography* 77.1 (2025), pp. 79–97. DOI: [10.16993/tellusa.4101](https://doi.org/10.16993/tellusa.4101).
- [7] A. Barzandeh, M. Rus, M. Ličer, I. Maljutenko, J. Elken, P. Lagema, and R. Uiboupin. “Application of HIDRA2 Deep Learning Model for Sea Level Forecasting Along the Estonian Coast of the Baltic Sea”. In: *EGUsphere* (2024). DOI: [10.5194/egusphere-2024-3691](https://doi.org/10.5194/egusphere-2024-3691).
- [8] C. Heuzé, L. Carlstedt, L. Poropat, and H. Reese. “Drivers of high frequency extreme sea level around Northern Europe - Synergies between recurrent neural networks and Random Forest”. In: *Ocean Science* tbd (2025), tbd. DOI: [update](https://doi.org/10.5194/egusphere-2024-3691).
- [9] P. Woodworth, J. Hunter, M. Marcos, P. Caldwell, M. Menéndez, and I. Haigh. “Towards a global higher-frequency sea level dataset”. In: *Geoscience Data Journal* 3.2 (2016), pp. 50–59. DOI: [10.1002/gdj3.42](https://doi.org/10.1002/gdj3.42).
- [10] I. D. Haigh, M. Marcos, S. A. Talke, P. L. Woodworth, J. R. Hunter, B. S. Hague, A. Arns, E. Bradshaw, and P. Thompson. “GESLA Version 3: A major update to the global higher-frequency sea-level dataset”. In: *Geoscience Data Journal* 10.3 (2023), pp. 293–314. DOI: [10.1002/gdj3.174](https://doi.org/10.1002/gdj3.174).
- [11] D. Codiga. *UTide Unified Tidal Analysis and Prediction Functions*. [package] MATLAB Central File Exchange. 2024. URL: <https://www.mathworks.com/matlabcentral/fileexchange/46523-utide-unified-tidal-analysis-and-prediction-functions>.
- [12] H. Hersbach, B. Bell, P. Berrisford, S. Hirahara, A. Horányi, J. Muñoz-Sabater, J. Nicolas, C. Peubey, R. Radu, D. Schepers, and A. Simmons. “The ERA5 global reanalysis”. In: *Quarterly Journal of the Royal Meteorological Society* 146.730 (2020), pp. 1999–2049. DOI: [10.1002/qj.3803](https://doi.org/10.1002/qj.3803).
- [13] T. Mauritsen, J. Bader, T. Becker, J. Behrens, M. Bittner, R. Brokopf, V. Brovkin, M. Claussen, T. Crueger, M. Esch, and I. Fast. “Developments in the MPI-M Earth System Model version 1.2 (MPI-ESM1.2) and its response to increasing CO<sub>2</sub>”. In: *Journal of Advances in Modeling Earth Systems* 11 (2019). DOI: [10.1029/2018MS001400](https://doi.org/10.1029/2018MS001400).
- [14] K.-H. Wieners, M. Giorgetta, J. Jungclaus, C. Reick, M. Esch, M. Bittner, S. Legutke, M. Schupfner, F. Wachsman, V. Gayler, H. Haak, P. de Vrese, T. Raddatz, T. Mauritsen, J.-S. von Storch, J. Behrens, V. Brovkin, M. Claussen, T. Crueger, I. Fast, S. Fiedler, S. Hagemann, C. Hohenegger, T. Jahns, S. Kloster, S. Kinne, G. Lasslop, L. Kornbluh, J. Marotzke, D. Matei, K. Meraner, U. Mikolajewicz, K. Modali, W. Müller, J. Nabel, D. Notz, K. Peters-von Gehlen, R. Pincus, H. Pohlmann, J. Pongratz, S. Rast, H. Schmidt, R. Schnur, U. Schulzweida, K. Six, B. Stevens, A. Voigt, and E. Roeckner. *MPI-M MPI-ESM1.2-LR model output prepared for CMIP6 CMIP historical*. 2019. DOI: [10.22033/ESGF/CMIP6.6595](https://doi.org/10.22033/ESGF/CMIP6.6595). URL: <https://doi.org/10.22033/ESGF/CMIP6.6595>.
- [15] D. Neubauer, S. Ferrachat, C. Siegenthaler-Le Drian, J. Stoll, D. S. Folini, I. Tegen, K.-H. Wieners, T. Mauritsen, I. Stemmler, S. Barthel, I. Bey, N. Daskalakis, B. Heinold, H. Kokkola, D. Partridge, S. Rast, H. Schmidt, N. Schutgens, T. Stanelle, P. Stier, D. Watson-Parris, and U. Lohmann. *IPCC DDC: HAMMOZ-Consortium MPI-ESM1.2-HAM model output prepared for CMIP6 ScenarioMIP ssp370*. 2023. DOI: [10.26050/WDC/AR6.C6SPHCME1s370](https://doi.org/10.26050/WDC/AR6.C6SPHCME1s370). URL: <https://doi.org/10.26050/WDC/AR6.C6SPHCME1s370>.
- [16] D. Neubauer, S. Ferrachat, C. Siegenthaler-Le Drian, J. Stoll, D. S. Folini, I. Tegen, K.-H. Wieners, T. Mauritsen, I. Stemmler, S. Barthel, I. Bey, N. Daskalakis, B. Heinold, H. Kokkola, D. Partridge, S. Rast, H. Schmidt, N. Schutgens, T. Stanelle, P. Stier, D. Watson-Parris, and U. Lohmann. *HAMMOZ-Consortium MPI-ESM1.2-HAM model output prepared for CMIP6 CMIP*. 2023. URL: <https://hdl.handle.net/21.14106/b9d7bdb67f42f35f7f73ff14a7fe439c3a1378a192>.
- [17] K.-H. Wieners, M. Giorgetta, J. Jungclaus, C. Reick, M. Esch, M. Bittner, V. Gayler, H. Haak, P. de Vrese, T. Raddatz, T. Mauritsen, J.-S. von Storch, J. Behrens, V. Brovkin, M. Claussen, T. Crueger, I. Fast, S. Fiedler, S. Hagemann, C. Hohenegger, T. Jahns, S. Kloster, S. Kinne, G. Lasslop, L. Kornbluh, J. Marotzke, D. Matei, K. Meraner, U. Mikolajewicz, K. Modali, W. Müller, J. Nabel, D. Notz, K. Peters-von Gehlen, R. Pincus, H. Pohlmann, J. Pongratz, S. Rast, H. Schmidt, R. Schnur, U. Schulzweida, K. Six, B. Stevens,

- 505 A. Voigt, and E. Roeckner. *IPCC DDC: MPI-*  
506 *M MPIESM1.2-LR model output prepared for*  
507 *CMIP6 ScenarioMIP*. 2023. DOI: [10.26050/](https://doi.org/10.26050/WDC/AR6.C6SPMXML2)  
508 [WDCC/AR6.C6SPMXML2](https://doi.org/10.26050/WDC/AR6.C6SPMXML2). URL: [https://doi.](https://doi.org/10.26050/WDC/AR6.C6SPMXML2)  
509 [org/10.26050/WDC/AR6.C6SPMXML2](https://doi.org/10.26050/WDC/AR6.C6SPMXML2).
- 510 [18] S. Hochreiter. *Long Short-term Memory*. Neu-  
511 ral Computation MIT-Press, 1997.
- 512 [19] F. Chollet and The Keras Team. *Keras*. [pack-  
513 age] Github. 2015. URL: [https://github.](https://github.com/fchollet/keras)  
514 [com/fchollet/keras](https://github.com/fchollet/keras).
- 515 [20] F. Lehner, C. Deser, N. Maher, J. Marotzke,  
516 E. M. Fischer, L. Brunner, R. Knutti, and  
517 E. Hawkins. “Partitioning climate projection  
518 uncertainty with multiple large ensembles and  
519 CMIP5/6”. In: *Earth System Dynamics* 11.2  
520 (2020), pp. 491–508. DOI: [10.5194/esd-11-](https://doi.org/10.5194/esd-11-491-2020)  
521 [491-2020](https://doi.org/10.5194/esd-11-491-2020).
- 522 [21] I. 2023. *IPCC, 2023: Summary for Policy-*  
523 *makers*. Ed. by H. Lee and J. Romero. IPCC,  
524 Geneva, Switzerland: Climate Change 2023:  
525 Synthesis Report. Contribution of Working  
526 Groups I, II and III to the Sixth Assessment  
527 Report of the Intergovernmental Panel on Cli-  
528 mate Change, 2023. DOI: [10.59327/IPCC/](https://doi.org/10.59327/IPCC/AR6-9789291691647.001)  
529 [AR6-9789291691647.001](https://doi.org/10.59327/IPCC/AR6-9789291691647.001).
- 530 [22] J. P. Dunne, H. T. Hewitt, J. Arblaster, F.  
531 Bonou, O. Boucher, T. Cavazos, P. J. Du-  
532 rack, B. Hassler, M. Juckes, T. Miyakawa, et  
533 al. “An evolving Coupled Model Intercompar-  
534 ison Project phase 7 (CMIP7) and Fast Track  
535 in support of future climate assessment”. In:  
536 *EGUsphere* 2024 (2024), pp. 1–51. DOI: [10.](https://doi.org/10.5194/egusphere-2024-3874)  
537 [5194/egusphere-2024-3874](https://doi.org/10.5194/egusphere-2024-3874).
- 538 [23] M. Schindelegger, J. Green, S. Wilmes, and  
539 I. Haigh. “Can we model the effect of observed  
540 sea level rise on tides?” In: *Journal of Geophys-*  
541 *ical Research: Oceans* 123 (2018), pp. 4593–  
542 4609. DOI: [10.1029/2018JC013959](https://doi.org/10.1029/2018JC013959).